

Faraday Discussions

Accepted Manuscript



This manuscript will be presented and discussed at a forthcoming Faraday Discussion meeting. All delegates can contribute to the discussion which will be included in the final volume.

Register now to attend! Full details of all upcoming meetings: <http://rsc.li/fd-upcoming-meetings>



This is an *Accepted Manuscript*, which has been through the Royal Society of Chemistry peer review process and has been accepted for publication.

Accepted Manuscripts are published online shortly after acceptance, before technical editing, formatting and proof reading. Using this free service, authors can make their results available to the community, in citable form, before we publish the edited article. We will replace this *Accepted Manuscript* with the edited and formatted *Advance Article* as soon as it is available.

You can find more information about *Accepted Manuscripts* in the [Information for Authors](#).

Please note that technical editing may introduce minor changes to the text and/or graphics, which may alter content. The journal's standard [Terms & Conditions](#) and the [Ethical guidelines](#) still apply. In no event shall the Royal Society of Chemistry be held responsible for any errors or omissions in this *Accepted Manuscript* or any consequences arising from the use of any information it contains.

ARTICLE

Hybrid organic semiconductor lasers for bio-molecular sensing

Cite this: DOI: 10.1039/x0xx00000x

A.-M. Haughey,^a C. Foucher,^a B. Guilhabert,^a A. L. Kanibolotsky,^b
P. J. Skabara,^b G. Burley,^b M. D. Dawson^a and N. Laurand^aReceived 00th January 2012,
Accepted 00th January 2012

DOI: 10.1039/x0xx00000x

www.rsc.org/

Bio-functionalised luminescent organic semiconductors are attractive for biophotonics because they can act as efficient laser materials while simultaneously interacting with molecules. In this paper, we present and discuss a laser biosensor platform that utilises a gain layer made of such an organic semiconductor material. The simple structure of the sensor and its operation principle are described. Nanolayer detection is shown experimentally and analysed theoretically in order to assess the potential and the limits of the biosensor. The advantage conferred by the organic semiconductor is explained and comparisons to laser sensors using alternative dye-doped materials are made. Specific biomolecular sensing is demonstrated and routes to functionalisation with nucleic acid probes, and future developments opened up by this achievement, are highlighted. Finally, attractive formats for sensing applications are mentioned, as well as colloidal quantum dots, which could in the future be used in conjunction with organic semiconductors.

A Introduction

The development of personalised medicine requires that specific diagnostic tools be made available for use at the point-of-care. In particular, sensitive and compact platforms that can flexibly and accurately identify disease biomarkers, e.g. from a patient's blood sample, and do so in the shortest time are critically needed.^{1,2} These diagnostic platforms should be simple to implement and operate in order to maximise practicality and minimise overall cost. Label-free optical biosensors enabled by advanced functional materials, including bio-functionalised organics, have the potential to address the challenge. Here, we describe an organic semiconductor (OS) laser as a technology platform for such label-free biosensing. Label-free biosensors in general use evanescent optical waves in order to measure minute changes in the dielectric permittivity caused by the presence of analytes at an interface between the device and the biological environment.³⁻¹¹ Such sensors are attractive because of their non-electrical detection, sensitivity and specificity. Several label-free optical sensor technologies currently exist.³ Each has its advantages and downsides but not all of them are easily scalable to the level of miniaturisation required for future point-of-care use. It is often necessary to sacrifice detection resolution and/or sensitivity for ease of implementation and vice-versa. This is because the

transduction mechanisms for reading the dielectric permittivity changes, i.e. for sensing, are based on resonating structures.³⁻¹¹

The sensing function is realised by monitoring the change of an optical resonance, for example by direct reading of the optical spectrum. The overall sensitivity of such sensor systems is then a combination of the magnitude of a resonance shift (caused by the presence of analytes) and of the intrinsic resonance bandwidth, which determines the minimum detectable shift. Optimising the sensitivity of an evanescent wave biosensor therefore means maximising the resonance shift (which can be done by maximising the optical wave intensity in the region where the analytes are present) while minimising the resonance bandwidth. Doing both simultaneously is not straightforward, as there exists a trade-off between resonance bandwidth and the strength of the wave/analyte interaction.

A plastic laser sensor platform, that can take the form of a distributed feedback^{12,13} or a photonic-crystal active resonator,¹⁴⁻¹⁵ can mitigate this trade-off while maintaining a simple architecture for ease of application. In such a device the narrow resonance bandwidth is obtained through the coherence of laser action without sacrificing the strength of the field (in this case the laser mode) interaction with the sensing region. The great potential of this solution for the detection of bio-molecules has been shown. However, the first generation of plastic laser sensors utilised a dye-doped composite, i.e. dyes

diluted in a polymeric matrix, as the optical gain region. The relatively low dielectric permittivity contrast between such a diluted medium ($n \approx 1.5$) and a biological environment ($n \approx 1.4$) limits the strength of the laser mode intensity at the sensing interface. Therefore, the approach necessitates the addition of a thin inorganic layer (TiO_2 , $n \approx 1.8$ to 2.4) on top of the surface of the laser to boost the field at the interface and hence the sensitivity. This additional step adds complexity to the fabrication and means that it is not entirely done by solution processing thereby cancelling some of the advantages of the technology.

We propose a novel embodiment of the plastic laser sensor where the laser material is made of a neat OS medium. This approach leads to a simple device architecture where no additional inorganic layer is necessary to obtain high sensing performance¹⁶⁻¹⁷ thanks to the relatively high dielectric permittivity of the dense OS medium. In turn, the fabrication of sensors can be entirely based on solution-processing techniques. Importantly for point-of-care, an OS laser configuration can be made suitable for compact optical-pumping arrangements using either InGaN laser diodes or LEDs¹⁸⁻²⁰ – thereby paving the way for miniaturisation of the biosensor system. Other key attributes of the OS laser biosensor include (i) wavelength flexibility across the visible by molecular engineering of the OS material – an attractive feature for multiplexing; (ii) compatibility with a variety of material platforms, thereby facilitating integration in legacy sensing equipment as well as the development of new sensor formats; and (iii) the possibility to envision direct hybridisation of the OS material at the molecular level to combine the functionalities of light amplification with those of bio-molecular interactions.

In this paper, we start in part B by presenting the design, concept and characteristics of the OS laser biosensor. In part C, we show that this laser platform can detect a nanolayer that is adsorbed onto the surface of the OS and explain the sensitivity advantage of using a dense OS as the gain medium. In part D, we demonstrate specific bio-molecular sensing, show DNA functionalisation of the OS laser and discuss opportunities opened up by these demonstrations. We briefly discuss possible OS lasers in array-format that are attractive for implementing particular sensing concepts. We end by mentioning another promising solution-processed material for hybrid laser biosensors, colloidal quantum dots, which could in the future be used in conjunction with OS.

B Organic laser sensor: design, materials and concept

The OS laser sensor considered here is based on a planar distributed-feedback structure as shown in Fig. 1(a). It consists of a transparent, nanopatterned substrate overcoated with a thin-film of OS that acts as the laser material and provides the interface with the sensing region. For sensing, the OS layer is put into contact with the biological environment (e.g. a drop of fluid to be tested can simply be deposited or flowed over the laser surface). The laser mode oscillates in the plane of the OS

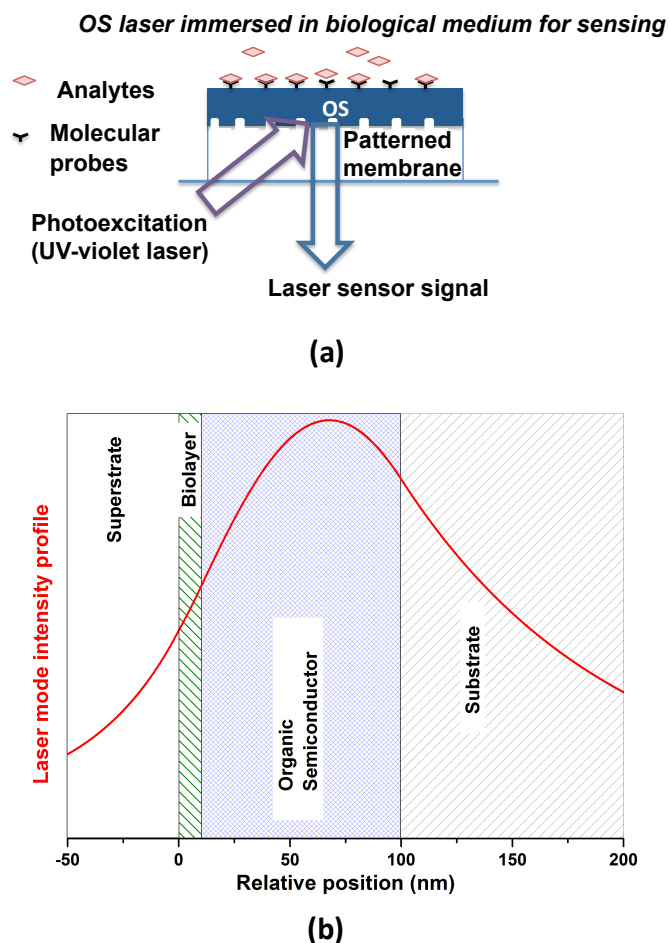


Fig. 1 (a) Schematic representing the implementation of the organic laser sensor; (b) laser mode intensity cross-section showing the overlap with the different regions of the laser structure.

layer and, as can be seen in Fig. 1(b), interacts with the biological environment ('superstrate' and 'biolayer') through its evanescent tails. The red curve in Fig 1(b) represents the laser mode intensity profile overlapped with the different regions of the planar laser. For ease-of-implementation, the nanopattern period is chosen to equal one wavelength of the desired laser emission. This laser emission has a vertically outcoupled component that can be collected for detection through the substrate of the device, i.e. on the same side as the pump excitation (Fig 1a). For biosensing, the sensor needs to be able to detect analytes specifically. Therefore, the surface of the laser is functionalised with molecular probes whose role is to capture and immobilise the molecules to be detected that might be present in the biological medium. Once captured, these immobilised analytes form a (possibly non-homogeneous) layer on the laser surface. The dielectric permittivity of this 'biolayer' is slightly higher than the more diluted biological medium, referred to as the superstrate in Fig. 1(b). This in turn affects the laser wavelength, which can be monitored for biosensing.

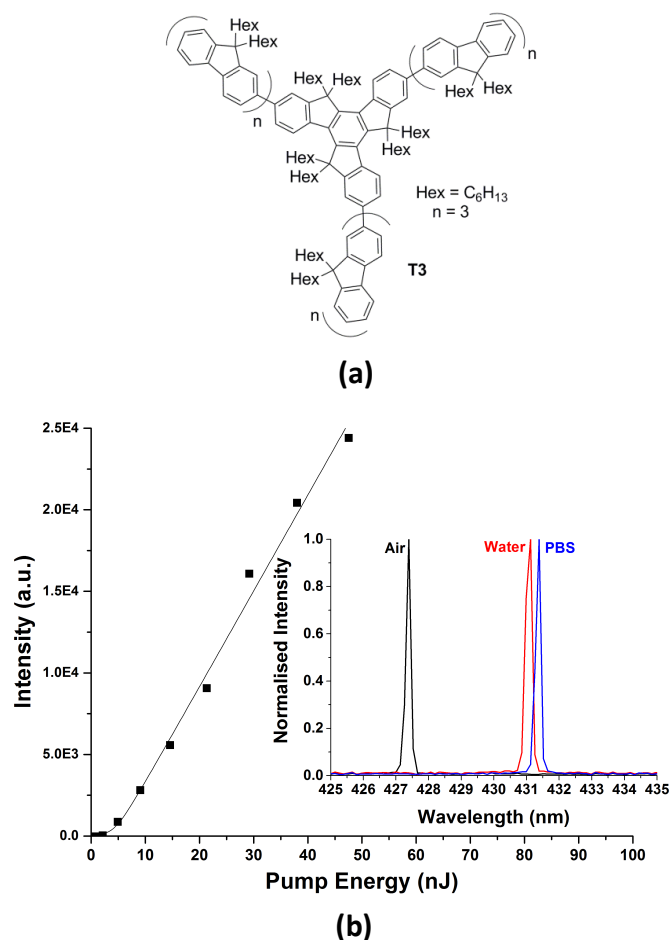


Fig. 2 (a) Representation of the T3 molecule; (b) Laser transfer function (in air); Inset: Laser spectrum with the superstrate being, respectively, air, water and PBS.

The laser wavelength is basically given by the product of the pattern periodicity, Λ , with the value of the mode effective index, n_{eff} . The latter is obtained by averaging the refractive indices of the substrate, OS, bilayer and superstrate weighted by the respective overlap values of these regions with the laser mode. The formation of a bilayer on the surface of the laser modifies the effective index and hence changes the laser wavelength. The magnitude of this change is dependent on the mode overlap with the bilayer and the refractive index of the latter. Hence, it depends on the amount of analyte and monitoring the wavelength enables the sensing function (although other parameters could be monitored as well). The mode overlap with the bilayer can be optimised for sensitivity by maximising the refractive index of the laser gain material and minimising its thickness. An OS laser material is therefore advantageous because it forms a ‘dense’ laser medium that has a high refractive index and can accommodate a low thickness without compromising the laser performance.

We use star-shape oligofluorene truxene molecules to form the OS layer of our laser sensors (see Fig. 2a). Each of the three arms of the molecule, attached to a truxene core, consists of a

repeat of fluorene units.²¹ In our case the number of units per arm is three and we therefore refer to this truxene-core material as T3. T3 macromolecules are efficiently excited with light in the 350-390nm range and emit in the blue part of the spectrum. They can also form high-quality solid-state thin-films with high T3 density ideal for planar lasers.^{22,23} The thickness of the T3 layer is set to be 70 nm +/- 10 nm, thin enough to maximise sensitivity and thick enough to sustain a TE-polarised optical mode. This layer of T3 is deposited onto a nanopatterned imprinted epoxy substrate. The periodicity of the pattern is $\Lambda=277$ nm. Such all-organic lasers can be easily incorporated into cuvettes or integrated into microtiter plates.

The laser sensors are excited with 5ns long pulses of 355nm pump light. A typical laser transfer function of such a laser (operated in air) is plotted in Fig. 2b. Despite the low T3 thickness, the oscillation threshold is 5 nJ and this value is even lower (a couple of nJ) when the laser is operated in a liquid superstrate such as water or buffer. The top inset of Fig. 2 displays the laser spectra when the superstrate is, respectively, air, water and phosphate buffered saline (PBS). The laser linewidth is limited by the spectrometer resolution in the three cases. The laser wavelength is seen to redshift for increasing refractive index of the superstrate: $\Delta\lambda$ (air-to-water) = 3.73 +/- 0.06 nm and $\Delta\lambda$ (air-to-PBS) = 4.00 +/- 0.06 nm. The respective refractive index of air, water and PBS solution is approximately 1, 1.34 and 1.35. Measurements of refractive index changes of the superstrate in such a way are repeatable and have been used to measure the concentration of glycerol/water solutions and have served to validate the sensing approach.¹⁶

To operate as a biosensor the photostability of the OS laser over the duration of an experiment is critical. T3 lasers operated in air have a 1/e degradation dosage of 10 J/cm², while it is close to 20 J/cm² when operated in a water environment (see Fig. 3). In the experimental conditions of our sensor, this corresponds to more than 10 to 20x10⁵ pulses. Over such a number of pulses the oscillation wavelength does not vary. Because a single sensing measurement requires less than 10 to 20 pulses there

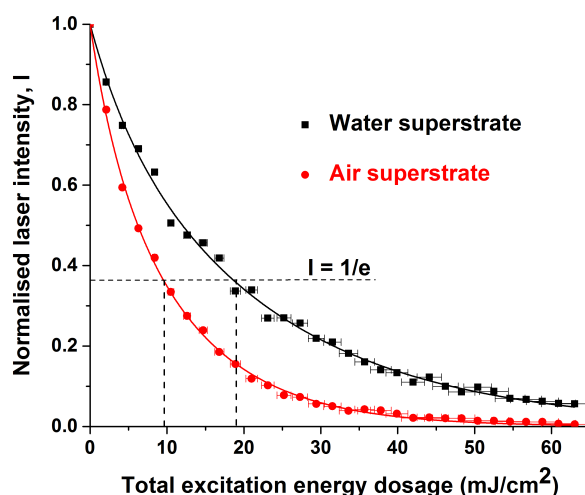
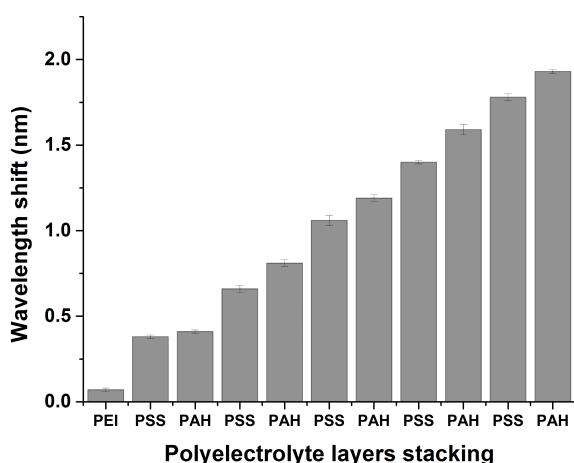


Fig. 3 Laser output intensity versus the total pump energy dosage when the device is operated in air and in water.

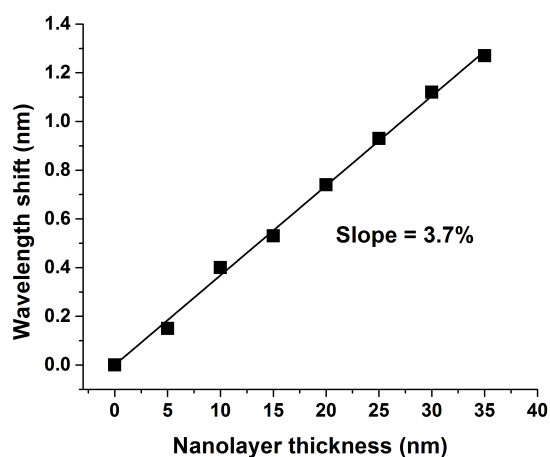
are no parasitic errors due to photodegradation effects. In fact, the T3 laser photostability is high enough that it should enable dynamic/continuous sensing over tens of minutes if exciting the laser sensor at a pulse repetition rate of 10 Hz.

C Nanolayer detection and comparison with dye-doped lasers

The biosensing principle of the laser platform is to detect molecules immobilised onto the surface of the OS material. This is different than sensing a change in the bulk refractive index of the superstrate as was shown in Fig. 2, inset. To observe the physical effect that a biolayer will have on the laser biosensor response, as well as to assess the capability and get a first idea of the sensing limit of the technology platform



(a)



(b)

Fig. 4 (a) Laser wavelength shift upon polyelectrolyte layers stacking. The first layer is made of PEI while each successively adsorbed polyelectrolytes are respectively PSS and PAH. **(b)** Laser wavelength shift versus adsorbed nanolayer thickness.

independently of biochemical surface functionalisation, nm-thick layers of polyelectrolytes can be built up onto the OS surface. For this, we use poly(ethyleneimine) (PEI), poly(allylamine hydrochloride) (PAH) and poly(sodium 4-styrenesulfonate) (PSS). These are well studied and form monolayers of known thickness (5 nm) and refractive index (1.49, close to that of most proteins) after a few initial layers of varying thicknesses.^{24,25} To adsorb each polyelectrolyte layer, the laser biosensor is immersed in solutions of the corresponding polyelectrolytes (all at 5 mg/mL in NaCl) for 10 minutes with intermediate washing steps. The first deposited layer is PEI and the successive layers forms a stack of PSS and PAH. After each layer deposition and surface washing, the laser wavelength is measured when immersed in a reference NaCl solution. The wavelength shift of the laser induced by this growth of nanolayers on top of the OS laser is shown in Fig. 4(a). After the first 3 layers, the wavelength redshifts linearly up to the 11th layer. The slope of the wavelength shift per nm of adsorbed material is 3.7% as indicated in Fig. 4(b). This means that the laser sensor can detect thicknesses of adsorbed material from the nanometre scale up to several tens of nanometres. In principle, the smallest thickness that could be detected is limited by the resolution of the current system (± 0.06 nm), corresponding to <2 nm. This equates to proteins in the range of 5 kDa,²⁶ i.e. the OS laser sensor has the potential to detect most of the relevant biomarkers. This assumes that proteins cover the whole of the laser surface, which might be the case only in the limit of high concentration. Nevertheless it demonstrates the intrinsic capability of the sensor while ignoring any amplification stage (that could be used to further boost the sensitivity).

Adsorption of a nanolayer is also a useful tool to compare

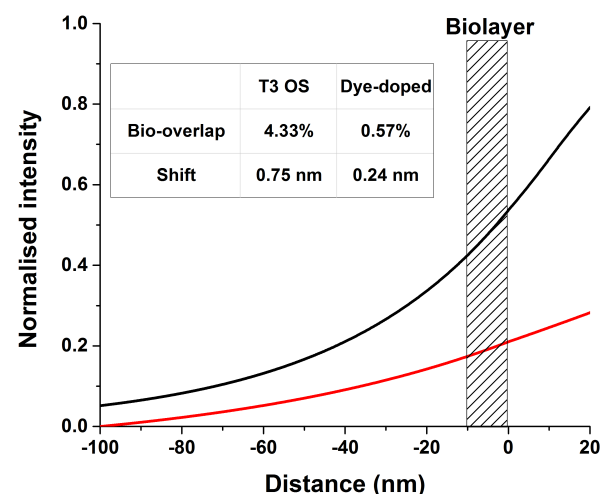


Fig. 5 Mode intensity profile in the vicinity of the laser/biolayer interface (position at 0 nm on graph). Red curve: case of the dye-doped laser; Black curve: case of the T3 OS laser. A 10nm thick biolayer is considered (patterned area between -10 nm and 0 nm). The mode overlap, and hence the wavelength shift, is higher for the T3 OS laser.

different surface sensing platforms independent of considerations for the chemistry of surface molecular probes. Here, we model our OS laser sensor and a similar laser structure that instead uses a dye-doped polymer for the gain region. Our model is based on a modified planar waveguide approach where we considered the dispersion of the different layers of the structure. This model has been shown to accurately predict and replicates experimental results for our OS laser.^{16,17} We have verified that it replicates published results of dye-doped laser sensors as well. We consider our T3 OS laser (details given previously) and a dye-doped laser emitting at 590 nm with a refractive index for the gain region of 1.51 and a pattern periodicity $\Lambda=400$ nm. The model determines in both cases the effective refractive index for the TE₀ mode, the mode profile, the overlap with the biolayer and the expected wavelength shift. The mode intensity profiles are represented in Fig. 5 along with the overlap values and the wavelength shifts for a 10nm biolayer with refractive index of 1.45. Both overlap and wavelength shifts are higher (4.37% vs 0.57% and 0.75 nm vs 0.24 nm) for the OS laser. The higher sensitivity of the OS laser is due to the higher index contrast between the laser and the biolayer. The dye-doped laser cannot match this sensitivity without an additional TiO₂ layer. Overall this section demonstrates that our T3 laser (and by extension other lasers made from neat OS) represents a simple yet potentially sensitive biosensing platform.

D Specific bio-molecular detection and DNA functionalisation

Specific detection of molecules requires surface functionalisation of the laser with molecular probes (Fig. 1a). We show, as proof-of-principle, specific detection of avidin by functionalising the T3 laser surface with biotin as the molecular probe. The approach for functionalisation utilises adsorption of a monolayer of a polyelectrolyte, polyphenylalanine lysine, or PPL (see inset of Fig. 6 for schematic representation of PPL). For this, a similar approach to layer adsorption described in section C was taken. Specifically, a solution of PPL in PBS (10 mM PBS, pH of 7.4) was prepared at a concentration of 1 mg/mL. The laser was immersed in this solution for 10 minutes and then washed and rinsed with PBS. The nanolayer of PPL provides accessible primary amine functional groups that can be used to anchor molecular probes on the laser surface. Here, the coated laser was immersed in a N-hydroxysuccinimide(NHS)-biotin/PBS solution for 20 minutes in order to attach biotin molecules onto the laser. The laser surface was then washed again in PBS. For sensing experiments, the biotin-functionalised laser was immersed in solutions of avidin/PBS of different concentrations for 20 minutes before a washing step to remove unbound avidin molecules.

Results of wavelength shift due to avidin attachment to the biotin laser as a function of avidin concentration are plotted in the main part of Fig. 6. Between 100 ng/mL and 1000 ng/mL the wavelength is seen to redshift with increasing avidin concentration. The behaviour saturates at a concentration

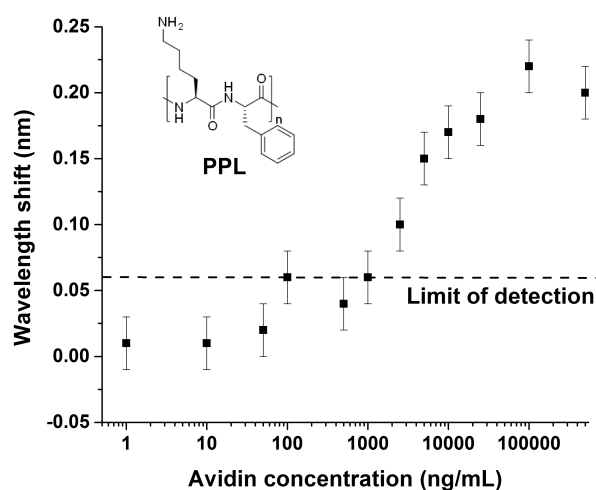


Fig. 6 Laser wavelength shift caused by avidin-biotin binding onto the laser surface as a function of avidin concentration. Inset: schematic of PPL monomer. PPL is used as an intermediate functionalisation layer on the T3 laser surface. It presents amine groups that are then reacted with NHS functionalised molecules (biotin here).

above 25 mg/mL. This saturating behaviour follows a Langmuir equation that relates to the coverage of molecules on a surface and is caused in this case by avidin molecules occupying all available biotin sites on the laser. The limit of detection corresponds to a concentration of 1000 ng/mL (shift of 0.06 nm). Currently, the limiting factor is the resolution of the system (convolution of the laser linewidth and of the spectrometer intrinsic resolution). Further refinement of the laser structure and the use of a spectrometer with a higher resolution will improve this limit of detection. We have also verified that this sensing capability is unaffected by the presence of albumin at a concentration equivalent to that found in blood.¹⁷ This is significant as albumin molecules tend to non-specifically stick to surfaces and this is known to cause problems in some biosensors.

This biomolecular sensing demonstration proves the potential of OS lasers for such applications. The next step is to devise functionalisation pathways for specific sensing of relevant biomarkers and to assess the limit of the technology in this case. The most common of commercial biosensors (e.g. ELISA assays) use antibodies but we think nucleic acid (NA) probes are well suited for functionalising OS lasers. NA probes have the advantage to be more environmentally stable than antigens/antibodies and they can also be synthetically programmed. With this approach the NA probes could immobilise on the laser surface the mRNA of protein biomarkers. Alternatively, aptamers could be used to directly immobilised proteins. As a first step on this route, we demonstrate NA attachment onto our T3 OS laser. We react an amide-to-maleimide crosslinker (Sulfosuccinimidyl-4-[N-maleimidomethyl]cyclohexane-1-carboxylate or SMCC) with

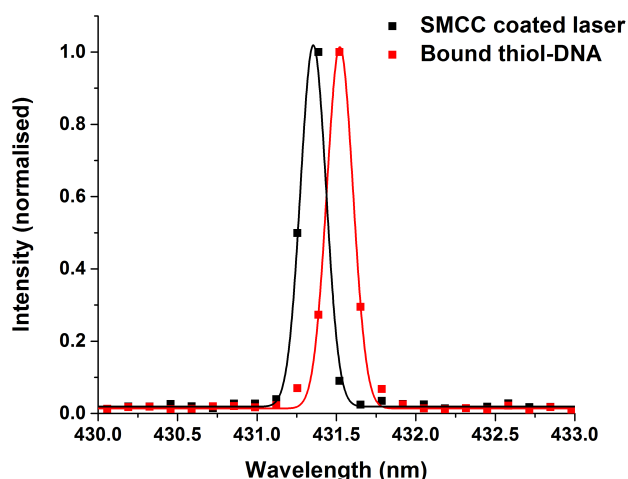


Fig. 7 Laser wavelength shift caused by binding of thiol-DNA onto the surface of an SMCC-coated laser.

the amine functional groups available onto the PPL-coated OS laser. This makes maleimide moieties available on the laser surface for further functionalisation. Fig. 7 represents the wavelength of such an SMCC functionalised laser before and after treatment with a solution of thiol-DNA. The shift (0.17 \pm 0.06 nm) is attributed to attachment of DNA onto the laser through the thiol-maleimide reaction. This represents a possible route to sensing with NA-probes.

An alternative and exciting avenue, albeit possibly synthetically challenging, will be to directly hybridise the NA probes with the OS molecules. Such a step, if viable, would enable an OS laser intrinsically bio-functionalised and 'sensing ready' after fabrication. This will create interesting opportunities for photonics and biochemistry and could lead to improved sensitivities.

Increasing the throughput of a biosensor can be obtained by (i) spatial multiplexing and by (ii) spectral multiplexing thereby enabling the parallel detection of different biomarkers. Both approaches could be combined. A possible way to realise spatial multiplexing is to have an array of OS lasers with each laser element being functionalised with a different type of molecular probes. The simplicity of the all-solution processing fabrication of the OS lasers lends itself to the assembly of such array of lasers. OS lasers in such a geometry compatible for integration with arrays of InGaN light-emitting diode excitation sources have been demonstrated.²⁷ Another way for spatial multiplexing is to functionalise a single OS laser, having a wide sensing area, with different molecular probes at different positions. Again, OS lasers are well suited for this as their active sensing area can be scaled from below 1 mm² up to several cm².¹³ Spectral multiplexing would enable simultaneous reading of closely assembled lasers, each emitting at a different wavelength. This will necessitate the use of lasers with different nanopattern periodicity as well as the use of different OS materials for further wavelength coverage.

We will end this paper by mentioning an alternative solution-processing material that could also be utilised for such laser

sensing in the future: colloidal quantum dots (CQDs). CQDs are inorganic semiconductor nanocrystals with surfaces that are coated with organic ligands. CQDs can cover a wide wavelength range (and are therefore attractive for spectral multiplexing) by tuning both the size of the CQDs and their alloy composition. The performance of optically-pumped CQD lasers is improving and their potential in format for sensing is real.^{28,29} Furthermore, CQD laser sensing will benefit from the advancing functionalities that are being developed for their use as bio-imaging labels. However, the threshold performance of CQD lasers is still two orders of magnitude higher than OS lasers and further improvement is needed. Nevertheless, it is a technology worth watching as in the future it could complement OS in such laser sensing applications.

Conclusions

Light-emitting organic semiconductors are already being investigated for gas sensing using their photoluminescent and/or optical gain properties.³⁰⁻³¹ Here, we see that they also have great potential for biosensing in a laser format. OS can act as the laser material as well as make the interface with the biological environment. The resulting OS lasers could lead to simple and compact label-free biosensing platforms. The DNA functionalization of an OS laser that is shown here opens up opportunities using the power of NA technology, both for device research and bio-applications. The challenge is now to assess the capability and limits of this approach in true applications. The all-solution-processing fabrication capability of OS lasers is one of their advantages. Other solution-based laser materials (e.g. CQDs) might have a role to play as well.

Acknowledgements

The authors would acknowledge the support of EPSRC for this work through the grant 'Hybrid Colloidal Quantum Dot Lasers for Conformable Photonics' (EP/J021962/1) and the platform grant 'Gallium nitride enabled hybrid and flexible photonics' (EP/I029141/1).

Notes and references

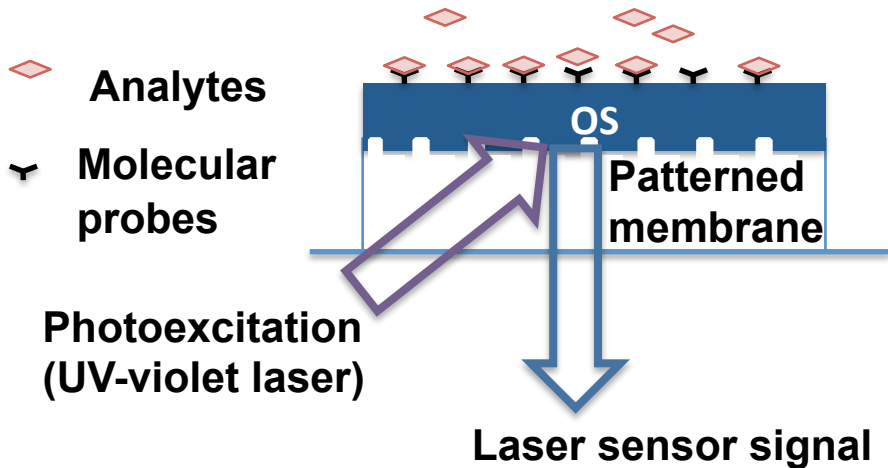
^a University of Strathclyde, Institute of Photonics, Glasgow, UK.

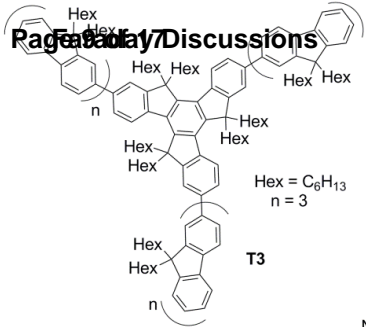
^b University of Strathclyde, WestCHEM, Department of Pure and Applied Chemistry, Glasgow, UK.

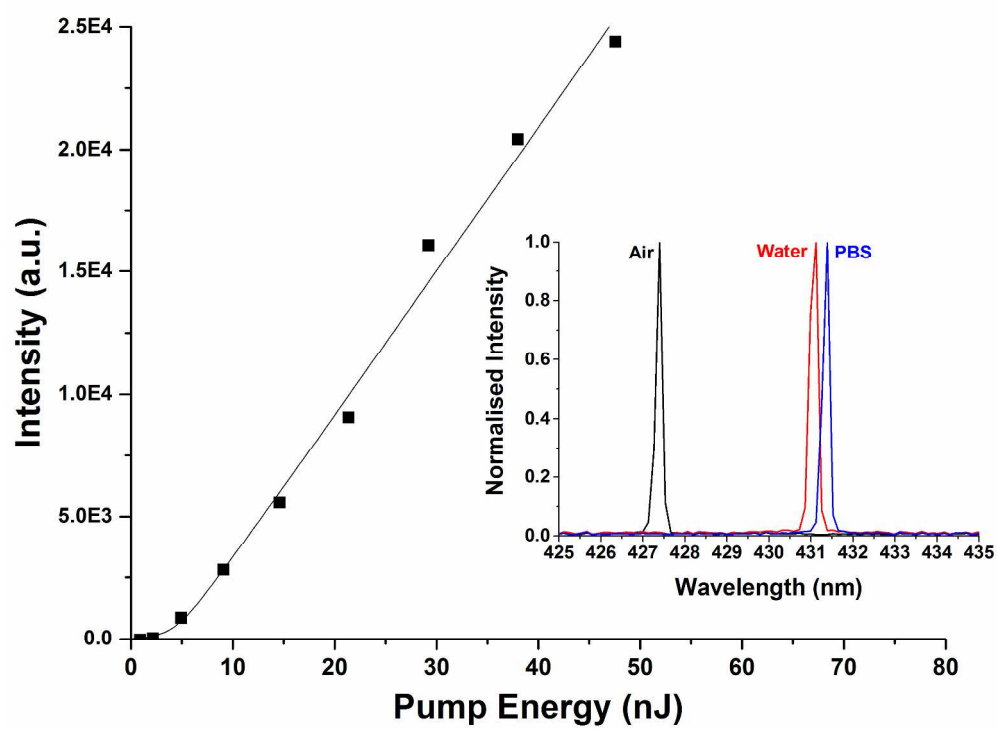
- 1 C. A. Holland and F. L. Kiechle, *Current Opinion in Microbiology*, 2005, **8**, 504-509.
- 2 A. J. Tudos, G. A. J. Besselink and R. B. M. Schasfoort, *Lab on a Chip*, 2001, **1**, 83-95.
- 3 X. Fan, I. M. White, S. I. Shopova, H. Zhu, J. D. Suter and Y. Sun, *Analytica Chimica Acta*, 2008, **620**, 8-26.
- 4 M. Kristensen, A. Krüger, N. Groothoff, J. García-Rupérez, V. Toccafondo, J. García-Castelló, M.J. Banuls, S. Peransi-Llopis, A.

- Maquieira, Optical Sensors, Optical Society of America, 2011, **SWB1** <http://www.opticsinfobase.org/abstract.cfm?URI=Sensors-2011-SWB1>.
- 5 S.M. Shamah and B.T. Cunningham, *Analyst*, 2011, **136**, 1090–1102.
- 6 V. Koubová, E. Brynda, L. Karasová, J. Škvor, J. Homola, J. Dostálek, P. Tobis`ka, J. Ros`icky´, *Sensors and Actuators B: Chemical*, 2001, **74**, 100–105.
- 7 M. Baaske and F. Vollmer, *ChemPhysChem*, 2012, **13**, 2, 427–436.
- 8 J. Homola, S.S. Yee and G. Gauglitz, *Sensors and Actuators B: Chemical*, 1999, **54**, 3–15.
- 9 B. Cunningham, J. Qiu, P. Li and B. Lin, *Sensors and Actuators B: Chemical*, 2002, **87**, 2, 365–370.
- 10 F. Volmer and S. Arnold, *Nature Methods*, 2008, **5**, 7, 591–596.
- 11 A.M. Armani, R.P. Kulkarni, S.E. Fraser, R.C. Flagan and K.J. Vahala, *Science*, 2007, **317**, 5839, (2007) 783–787.
- 12 M. Lu, S. S. Choi, C. J. Wagner, J. G. Eden and B. T. Cunningham, *Applied Physics Letters*, 2008, **92**, 26, 261502.
- 13 Y. Tan, C. Ge, A. Chu, M. Lu, W. Goldschlag, C. S. Huang, A. Pokhriyal, S. George, B. Cunningham, *IEEE Sensors Journal*, 2012, **12**, 5, 1174–1180.
- 14 C. L. C. Smith, J. U. Lind, C. H. Nielsen, M. B. Christiansen, T. Buss, N. B. Larsen, A. Kristensen, *Optics Letters*, 2011, **36**, 8, 1392–1394.
- 15 C. Vannahme, C. L. C. Smith, M. B. Christiansen and A. Kristensen, *Appl. Phys. Lett.*, 2012, **101**, 151123.
- 16 A.-M. Haughey, B. Guilhabert, A. L. Kanibolotsky, P. J. Skabara, G. A. Burley, M. D. Dawson and N. Laurand, *Sensors and Actuators B: Chemical*, 2013, **185**, 132–139.
- 17 A.-M. Haughey, B. Guilhabert, A. L. Kanibolotsky, P. J. Skabara, G. A. Burley, M. D. Dawson and N. Laurand, *Biosensors and Bioelectronics*, 2014, **54**, 679–686.
- 18 T. Riedl, T. Rabe, H.-H. Johannes, W. Kowalsky, J. Wang, T. Weimann, P. Hinze, B. Nehls, T. Farrell and U. Scherf, *Appl. Phys. Lett.*, 2006, **88**, 241116.
- 19 A. E. Vasdekis, G. Tsiminis, J.-C. Ribierre, L. O’Faolain, T. F. Krauss, G. A. Turnbull and I. D. W. Samuel, *Optics Express*, 2006, **14**, 20, 9211–9216.
- 20 Y. Yang, G. A. Turnbull, I. D. W. Samuel, *Applied Physics Letters*, 2008, **92**, 16, 163306.
- 21 A.L. Kanibolotsky, R. Berridge, P.J. Skabara, I.F. Perepichka, D.D.C. Bradley and M. Koeberg, *Journal of the American Chemical Society*, 2004, **126**, 42 13695–13702.
- 22 G. Tsiminis, Y. Wang, P.E. Shaw, A.L. Kanibolotsky, I.F. Perepichka, M.D. Dawson, P.J. Skabara, G.A. Turnbull and I.D.W. Samuel, *Applied Physics Letters*, 2009, **94**, 24, 243304–243304-3.
- 23 J. Herrnsdorf, B. Guilhabert, Y. Chen, A. Kanibolotsky, A. Mackintosh, R. Pethrick, P. Skabara, E. Gu, N. Laurand, M. D. Dawson, *Optics Express*, 2010, **18**, 25, 25535–25545.
- 24 J. Schmitt, T. Gruenewald, G. Decher, P.S. Pershan, K. Kjaer, M. Loesche, *Macromolecules*, 1993, **26**, 25, 7058–7063.
- 25 M. Lösche, J. Schmitt, G. Decher, W.G. Bouwman, K. Kjaer, *Macromolecules*, 1998, **31**, 25 8893–8906.
- 26 H.P. Erickson, *Biological Procedures Online*, 2009, **11**, 1, 32–51.
- 27 B. Guilhabert, N. Laurand, J. Herrnsdorf, Y. Chen, A. L. Kanibolotsky, C. Orofino, P. J. Skabara and M. D. Dawson, *IEEE Photonics Journal*, 2012, **4**, 3, 684–690.
- 28 B. Guilhabert, C. Foucher, A.-M. Haughey, E. Mutlugun, Y. Gao, J. Herrnsdorf, H. D. Sun, H. V. Demir, M. D. Dawson and N. Laurand, *Opt. Express*, 2014, **22**, 7308–7319.
- 29 C. Foucher, B. Guilhabert, N. Laurand and M.D. Dawson, *Appl. Phys. Lett.*, 2014, **104**, 14, 141108.
- 30 A. Rose, Z. Zhu, C. Madigan, T. Sager and V. Bulovic, *Nature*, 2005, **434**, 7035, 876–879.
- 31 Y. Yang, G. A. Turnbull and I. D. W. Samuel, *Advanced Materials*, 2010, **20**, 13, 2093–2097.

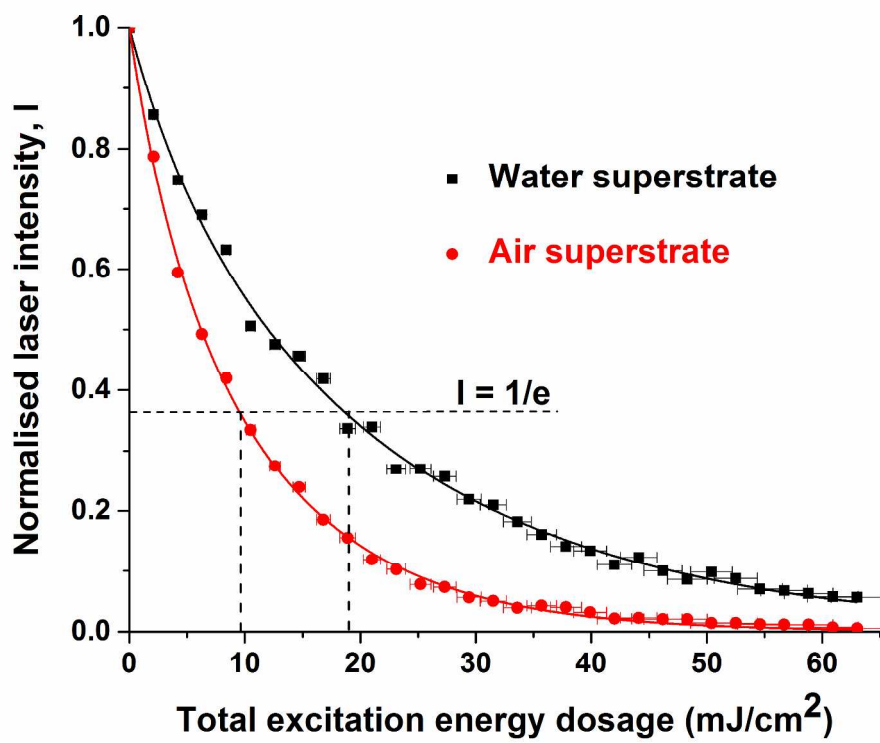
OS laser immersed in biological medium for sensing



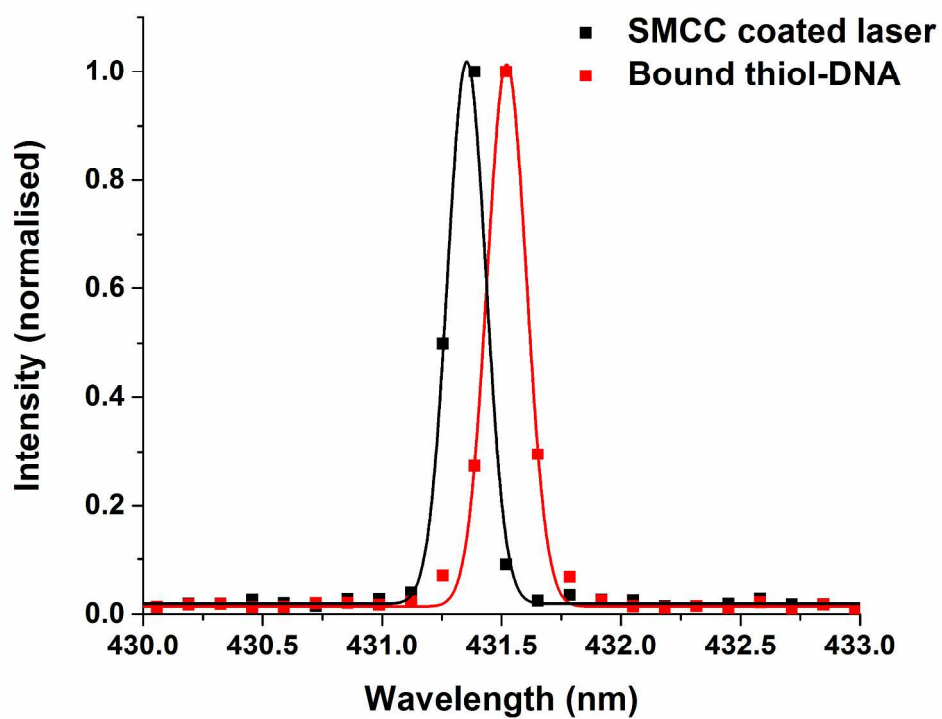




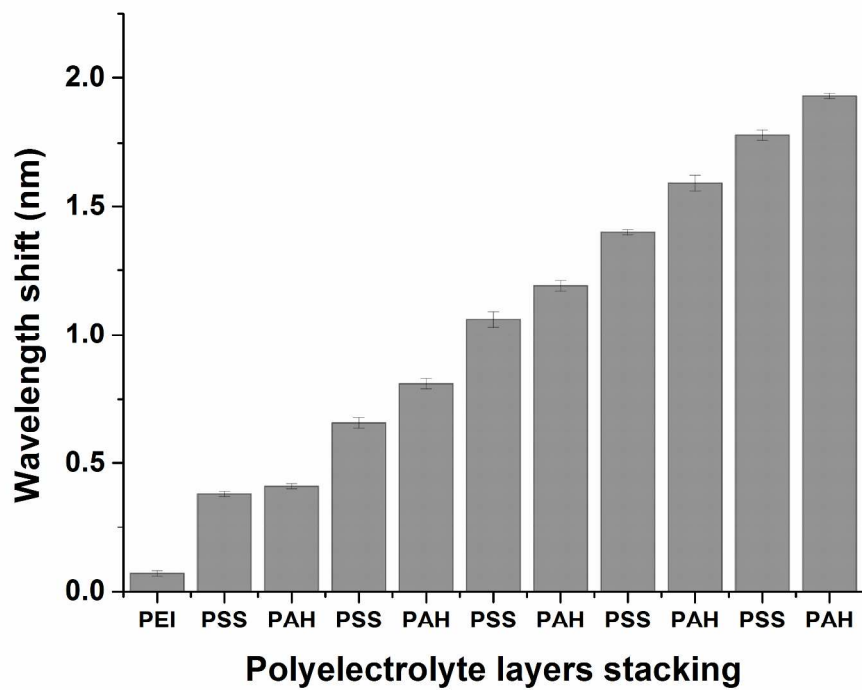
270x206mm (300 x 300 DPI)



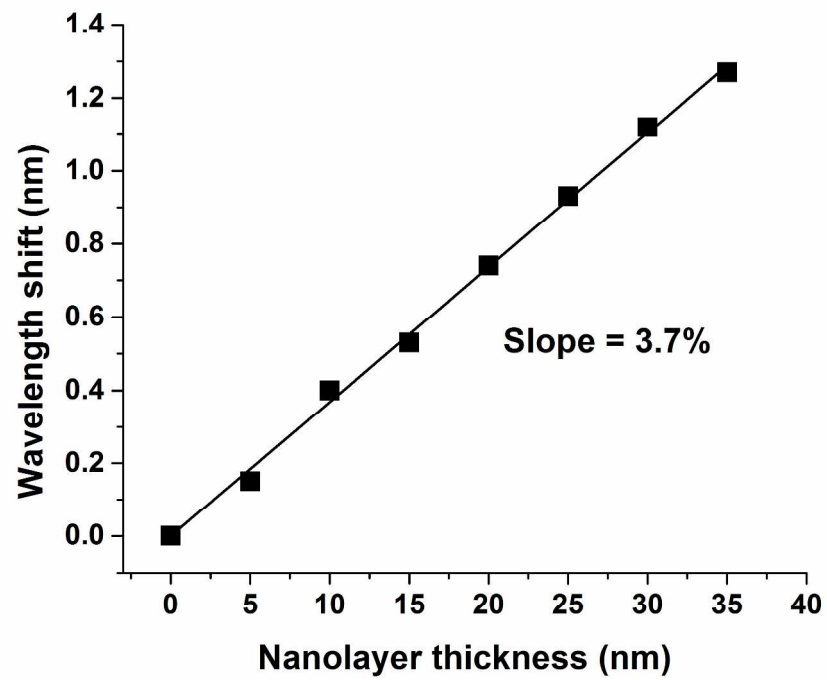
270x206mm (300 x 300 DPI)



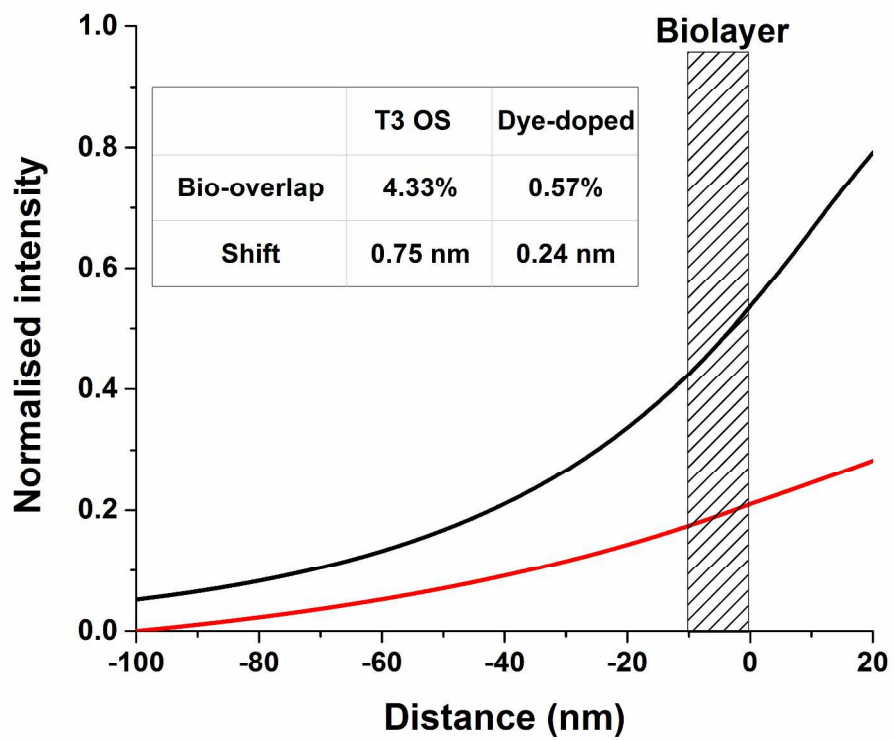
270x206mm (300 x 300 DPI)



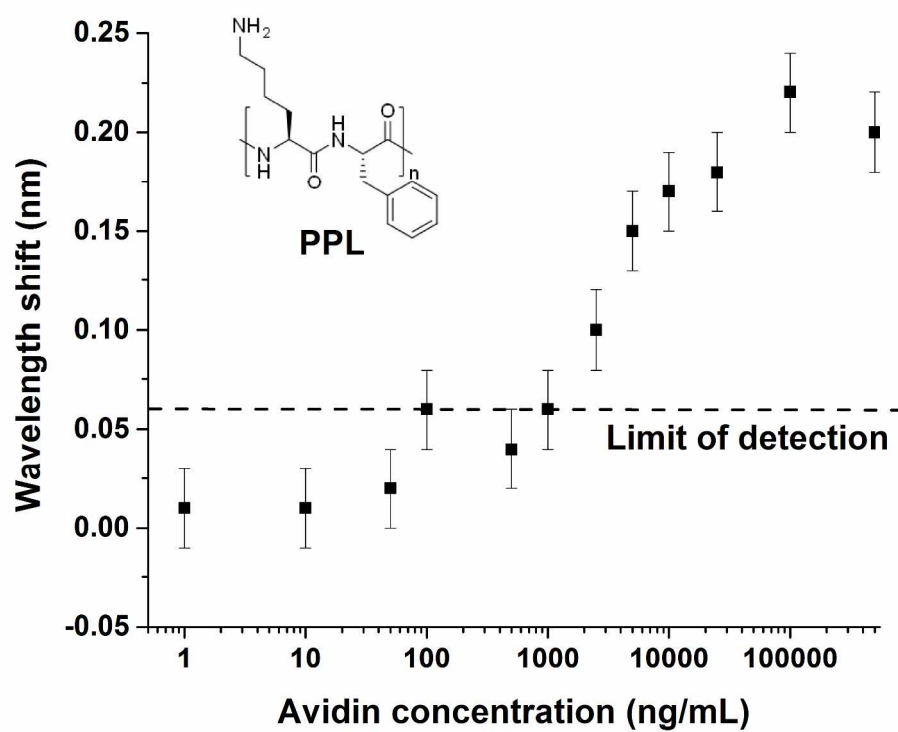
270x206mm (300 x 300 DPI)



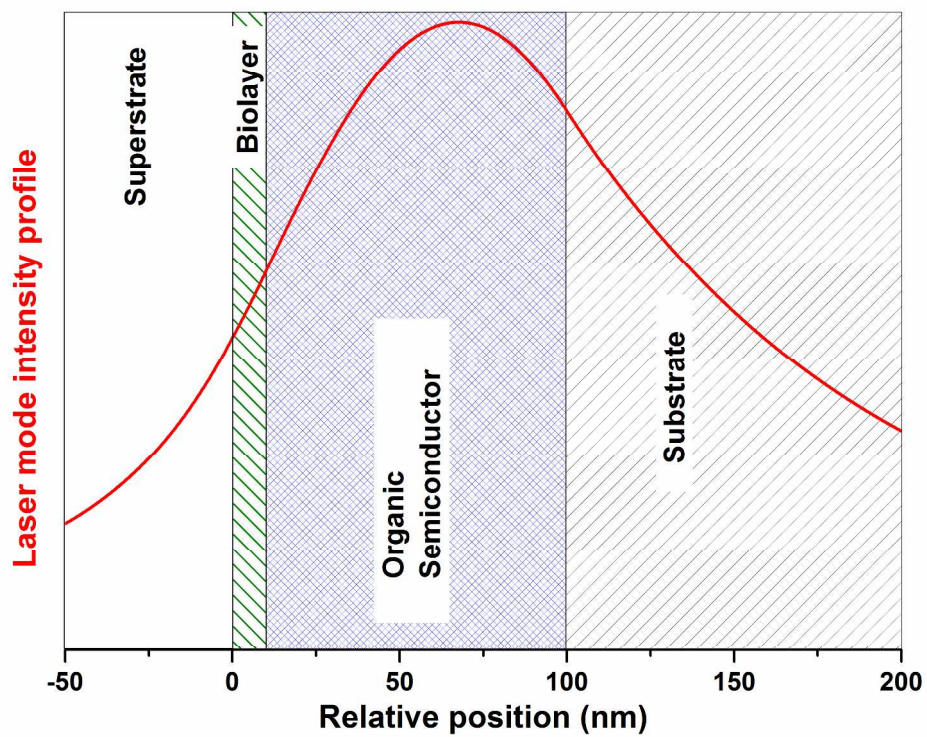
270x206mm (300 x 300 DPI)



270x206mm (300 x 300 DPI)



270x206mm (300 x 300 DPI)



270x206mm (300 x 300 DPI)